

X-Ray Reflectometry Study of the State of the Surface Layer of Polished Silicon Substrates Depending on the Methods of Their Cleaning

Yu. A. Volkovsky^{a, b, *}, A. Yu. Seregin^{a, b}, M. S. Folomeshkin^{a, b}, P. A. Prosekov^{a, b}, M. D. Pavlyuk^a,
Yu. V. Pisarevsky^{a, b}, A. E. Blagov^{a, b}, and M. V. Kovalchuk^{a, b, c}

^a Institute of Crystallography FSRC “Crystallography and Photonics”, Russian Academy of Sciences, Moscow, 119333 Russia

^b National Research Center “Kurchatov Institute”, Moscow, 123182 Russia

^c Saint Petersburg State University, Saint Petersburg, 199034 Russia

*e-mail: irlandez08@yandex.ru

Received January 22, 2021; revised March 25, 2021; accepted March 28, 2021

Abstract—The state of the surface layer of polished silicon substrates and the effect of surface-cleaning procedures, such as washing in an ultrasonic bath, etching, and vacuum annealing, is studied. The X-ray reflectivity technique is used to determine the root-mean-square (rms) roughness, thickness, and density of the damaged surface layer. It is shown that the substrates have a damaged surface layer 1.5 nm thick, which is most pronounced after annealing at 350°C. Based on the etching procedures and subsequent vacuum annealing, an approach is proposed for cleaning the surface from contaminants, the damaged layer, and obtaining substrates with a root-mean-square roughness of $\sigma_z = 0.42$ nm. This approach can be used, in particular, for the deposition of thin organic films.

Keywords: X-ray reflectivity, roughness, silicon substrate, surface, annealing, damaged layer

DOI: 10.1134/S1027451021050207

INTRODUCTION

Silicon wafers are widely used as a base for the formation of organic, hybrid films. They gained such popularity due to well-developed technologies for the fabrication of a smooth surface with ultra-low roughness and active studies of the surface morphology. In the microelectronics industry, where silicon substrates are used in production as one of the main materials, the growth and structure of silicon oxide on the wafer surface [1, 2] and the effect of surface preparation using polishing and etching procedures on its roughness are studied well [3]. The surface of such substrates is studied by various methods: atomic-force microscopy, ellipsometry, small-angle X-ray scattering [4], and X-ray reflectometry [5–7].

In recent years, technologies for the production and diagnostics of organic and hybrid planar systems have been actively developed, in particular, using the Langmuir technology of transferring layers onto solid substrates [8–13]. The specificity of such systems imposes additional requirements on the chemical purity and neutrality of the substrate surface in relation to the studied objects (layers), and ultrasonic baths and cleaners are widely used to this end [14]. The characteristic layer thicknesses in units of nanometers

make it necessary to use substrates with an appropriate surface smoothness.

There are a number of methods for the chemical cleaning of silicon substrates from organic and inorganic impurities and for the fabrication of a surface with a roughness no higher than 1.0–1.5 nm [15]. However, the use of such cleaning methods can lead to the formation of damaged surface layers. The scattering power of organic films, low or comparable with that of the substrate, requires taking into account the effect of the damaged surface layer, which complicates interpretation of the X-ray experimental results.

In this work, a reflectometry study of the effect of a number of surface-cleaning procedures (washing in an ultrasonic bath, etching and vacuum annealing) and their combinations on the structure of the surface layer of polished silicon substrates is carried out.

OBJECTS AND METHODS

Materials and Preparation of Test Samples

The substrates were single-crystal BPKZh 90.01.000 TU silicon wafers 380 ± 20 μm thick with one-sided chemical-mechanical polishing [16]. The surface cut deviated from the crystallographic direction [100] by $4^\circ \pm 0.5^\circ$ in the [110] direction. The size

of the wafers was 20×15 mm. The substrates were studied after vacuum annealing without preliminary cleaning, vacuum annealing after washing in an ultrasonic bath, and vacuum annealing after washing in an ultrasonic bath and etching.

Vacuum annealing of the samples was carried out in a thermal vacuum cell (Anton Paar, DHS-1100) with a dome transparent to X-ray radiation, mounted on an X-ray diffractometer. Heating was carried out in vacuum chamber with a residual pressure of 10^{-3} mbar at a rate of 3.6 deg/min. The surface was studied by X-ray reflectometry after the sample was heated to a predetermined temperature. Before the start of measurements, the sample was kept at the given temperature for 5 min. The samples were cooled (in vacuum) at a rate of 12 deg/min to room temperature after reaching the final annealing temperature, and then X-ray studies were also carried out.

Cleaning in an ultrasonic bath was carried out in an ultrapure ethanol solution at a temperature of 50°C for 1 h. Then the substrates were washed with ultrapure water (resistance of 18 MOhm cm) prepared using the Simplicity 185 system (Millipore). A jet of compressed air blew water off the substrate layer.

Etching was carried out using a polishing etchant in the form of an aqueous solution of 46% hydrofluoric acid with the addition of $\text{NiSO}_4 \cdot 7\text{H}_2\text{O}$ salt in the ratio 6.52 : 1 at a temperature of 25°C. The etching rate was ≈ 1 nm/s. After etching, the substrates were also washed with ultrapure water, and water was blown with a jet of compressed air.

X-Ray Reflectometry Method

The X-ray reflectometry experiments were carried out on a SmartLab diffractometer (Rigaku) equipped with a 9-kW X-ray source with a rotating molybdenum anode. The spectral $\text{MoK}_{\alpha 1}$ line ($\lambda = 0.70932$ Å) was used, and the beam intensity was recorded with a scintillation detector. To form a quasi-parallel beam, a Göbel multilayer mirror (CBO, Rigaku) was used. The angular resolution in the diffraction plane, provided by a system of incident and receiving slits, was 0.012° . An additional K_{β} filter was mounted in front of the detector to exclude the contribution of the X-ray spectral K_{β} line to the angular intensity distribution. In the transverse direction, the incident beam illuminated almost the entire sample. The reflectometry curve was recorded in the range of scattering vector q values of 0 – 10 nm^{-1} .

Analysis of the X-Ray Reflectometry Data

The following approach was used to analyze the experimental data. The sample under study was a layered system with a characteristic stepwise profile of the electron density distribution along the normal to the surface (along the depth). Each layer of such a system

differed in thickness and polarizability determined by the atomic composition. To take into account the imperfection of the interfaces (roughness, transition layer), the interface between the layers was set in the form of a smoothed error function.

The smoothed electron density profile constructed taking into account the transition layers was divided into elementary lamellas (sublayers). The thickness of the lamellas was chosen so that the change in the electron density could be neglected within the limits of their thickness. Theoretical calculation of the reflectometry curve for this model was carried out for the formed set of lamellas by the method of Parrett's recurrence relations [17]. By minimizing the function χ^2 , which characterizes the discrepancies between the experimental data and theoretical values, using the nonlinear least-squares method (Levenberg–Marquardt method [18]), the profiles of the electron density distributions over the depth of the surface region of the samples were obtained.

RESULTS AND DISCUSSION

Stepwise Vacuum Annealing without Preliminary Cleaning

The sample was heated in stages: with a step of 25 to 50°C and with a step of 50 to 150°C. After each heating stage, before starting the measurements, the sample was kept at the given temperature for 5 min. The time taken to record the reflectometry curve at a fixed temperature was 30 min.

A bilayer model (substrate/surface layer) was used to process the experimental data, since the simplest model, the substrate, did not allow description of the experimental dependence. Table 1 shows the results of processing the reflectometry curve: the calculated thickness d is indicated, the electron density ρ_e with respect to the substrate, the roughness σ_z and the χ^2 value are shown. The roughness of the surface layer of the initial substrate was 0.29 nm before annealing. When the heating temperature increased, the roughness decreased and the electron density of the surface region increased. The roughness $\Delta\sigma_z = 0.05$ nm and electron density varied most strongly in the temperature range from 50 to 100°C (Figs. 1a, 1b), which may be associated with the evaporation of water and light organic compounds. Subsequent heating to 150°C had little effect on the roughness of the surface layer.

After cooling the substrates to room temperature and the subsequent input of air into the thermal vacuum cell (Figs. 1b, 1d), an increase in the roughness of the surface layer is observed by $\Delta\sigma_z = 0.06$ to 0.28 nm, and an increase in the electron density to 0.90, which is possibly due to oxidation of the surface layer and contamination due to the input of air (atmosphere) into the cell. The change in the roughness of the surface layer before and after heating was 0.01 nm. Vac-

uum annealing at 150°C has little effect on the surface of the silicon substrate (Table 1).

*Stepwise Vacuum Annealing at 350°C
after Cleaning in an Ultrasonic Bath*

To clean the substrate from settled dust and light organic contaminants, it was washed in an ultrasonic bath in ethanol and then washed with distillate. After washing, the sample was subjected to stepwise heating to 350°C with a variable step: from 25 to 50°C with a step of 25°C, from 50 to 150°C with a step of 50°C, from 150 to 300°C with a step of 75°C and from 300 to 350°C with a step of 50°C. After each heating stage, before the start of measurements, the sample was exposed for 5 min. The time taken to record the reflectometry curve at a fixed temperature was 30 min. Table 2 shows the results of processing the angular intensity distribution using the bilayer model (substrate/surface

Table 1. Parameters of the model of the surface layer at stepwise vacuum annealing up to 150°C

Temperature, °C	d , nm	ρ_e	σ_z , nm	χ^2
25	1.1	0.89	0.29	1.5
50	1.1	0.90	0.27	1.6
100	0.7	0.85	0.22	1.8
150	0.8	0.88	0.22	1.8
After annealing	1.0	0.90	0.28	1.4

d is the surface-layer thickness, ρ_e is the electron density of the layer relative to the substrate, σ_z is the surface-layer roughness.

layer). It should be noted that after cleaning the sample in an ultrasonic bath, the layer roughness increased by 0.05 nm and the electron density of the surface region decreased compared to the sample without cleaning (Fig. 2a, 2b), which is due to the fact that

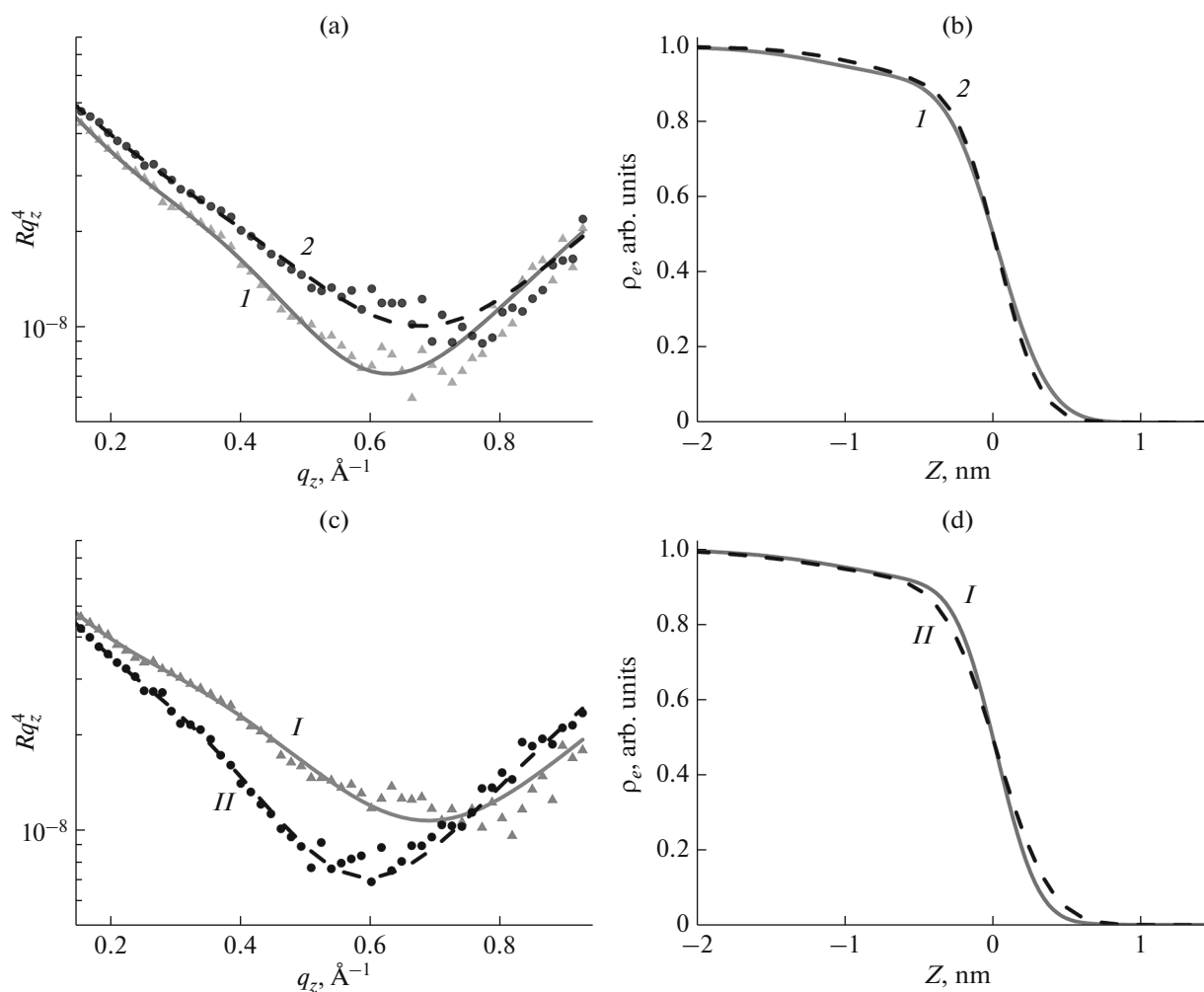


Fig. 1. Research results at stepwise vacuum annealing up to 150°C: (a, c) X-ray reflectometry curves; (b, d) corresponding electron density profiles over the sample depth upon heating to 50 (I), 100 (2), 150°C (I), after annealing (II). For clarity, the X-ray reflectometry curves are normalized to q_z^4 . Points—experiment, lines—calculation.

Table 2. Parameters of the model of the surface layer at stepwise vacuum annealing up to 350°C with preliminary cleaning in an ultrasonic bath

Temperature, °C	d , nm	ρ_e	σ_z , nm	χ^2
25	0.7	0.75	0.34	0.9
50	1.1	0.84	0.33	1.0
100	1.1	0.90	0.29	1.2
150	1.1	0.87	0.29	1.4
225	1.1	0.83	0.29	1.4
300	1.4	0.90	0.29	1.5
350	1.5	0.92	0.28	1.5
After annealing	1.8	0.95	0.30	1.1

d is the surface-layer thickness, ρ_e is the electron density of the layer with respect to the substrate, σ_z is the surface-layer roughness.

Table 3. Parameters of the model of the surface layer at one-stage vacuum annealing up to 350°C with preliminary cleaning in an ultrasonic bath

Temperature, °C	d , nm	ρ_e	σ_z , nm	χ^2
25	1.6	0.80	0.35	1.2
350	1.5	0.94	0.27	1.4
After annealing	1.5	0.91	0.29	1.0

d is the surface-layer thickness, ρ_e is the electron density of the layer relative to the substrate, σ_z is the surface-layer roughness.

readily soluble organic fractions were washed away from the substrate layer.

The character of the decrease in the roughness of the surface layer upon heating to 150°C (Table 2) is similar to that observed upon vacuum annealing without preliminary cleaning (Table 1). The roughness changes slightly upon heating from 150 to 300°C. In the range of 300–350°C, the density of the surface layer increases, which, together with a decrease in roughness, leads to the appearance of a layer-substrate interface in the electron-density-distribution profile in the form of a step (Figs. 2c, 2d). It can be assumed that this effect is due to the evaporation of volatile contaminants from the damaged surface layer of the sample. The thickness of such a layer is 1.5 nm.

After cooling the sample and the subsequent input of air into the thermal vacuum cell, the roughness slightly increased by 0.02 nm, and an increase in the thickness of the developed surface layer was also observed. One should note the difference in the change in the roughness of the samples in air after annealing. If for the sample without preliminary cleaning, the increase in roughness was 0.06 nm after vacuum annealing to 150°C, it was 0.02 nm for the sample after cleaning in an ultrasonic bath and annealing to 350°C. This indicates that less dust and organic contaminants from the atmosphere settle on

the surface of the substrate cleaned in an ultrasonic bath upon annealing to 350°C and filling the thermal vacuum cell with air than on the surface without preliminary cleaning and with a lower heating temperature.

The change in the roughness of the surface layer before and after annealing was 0.04 nm. It can be assumed that not only water evaporated from the sample surface after annealing, but also heavy contaminants were removed, which “washed away the pattern” near the boundary of the surface layer on the electron density profile, masking this layer.

One-Stage Vacuum Annealing at 350°C after Washing in an Ultrasonic Bath

Since the measurement time for one reflectometry curve is 30 min, it was of interest to carry out the experiment without recording the curve at intermediate temperatures. The sample was cleaned in an ultrasonic bath followed by continuous heating to 350°C without intermediate stages. The heating time was 1.5 h, and exposure at 350°C before recording the reflectometry curve was 5 min. The bilayer model (substrate/surface layer) was also used when processing the experimental data (Table 3).

The X-ray reflectometry data show a similar pattern of changes in the roughness and density of the surface layer of the sample at multi-stage and one-stage annealing up to 350°C. A “step” appears on the electron density profile reflecting a surface layer 1.5 nm thick. After cooling the sample, the roughness increased by 0.02 nm, the same as in the case of stepwise annealing (Table 2). In further studies, the samples were subjected to one-stage annealing.

One-Stage Vacuum Annealing after Ultrasonic Cleaning and Etching

In order to remove the damaged surface layer and evaporate volatile contaminants, the surface was etched, washed with distillate and then annealed at 350°C. The characteristic thickness of the damaged surface layer revealed during annealing is about 1.5 nm (Tables 2 and 3). Based on the thickness of the damaged layer and the concentration of the etching solution (etching rate \approx 1 nm/s), the etching times were chosen as 2, 4, 6, and 12 s.

A reflectometry curve was recorded at room temperature after etching. The presence of oscillations on the curves (Figs. 3a, 3b) indicates the formation of a layer about 1 nm thick on the surface of the substrates, which can be caused by residues of both the damaged surface layer and the etchant after washing the substrate layer with distillate. Therefore, a substrate/bicomponent layer model was used when processing the sample data after etching but before annealing. Table 4 shows the parameters of the layer model on the surface of substrates after etching with

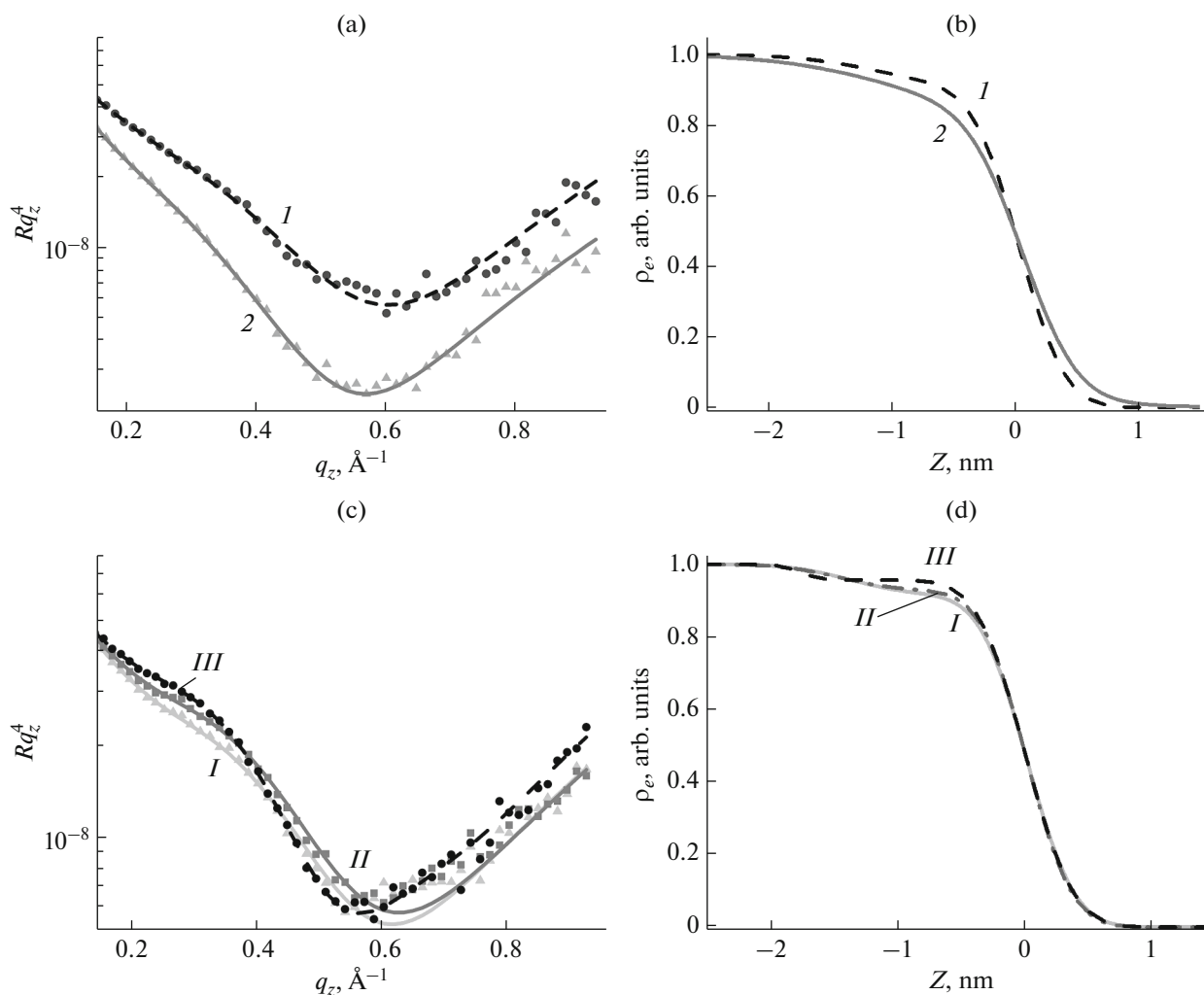


Fig. 2. Investigation results upon vacuum annealing up to 350°C after washing in an ultrasonic bath: (a, c) X-ray reflectometry curves; (b, d) corresponding electron density profiles over the sample depth without washing (*I*), with washing (*2*) at room temperature in a vacuum chamber, at heating to 300 (*I*), 350°C (*II*), after cooling (*III*). For clarity, the X-ray reflectometry curves are normalized to q_z^4 . Points—experiment, lines—calculation.

different exposure times according to X-ray reflectometry data obtained at room temperature. Since such a layer has a complex structure, when the etching time increases from 2 to 4 s, its thickness first decreases due to the component corresponding to the residues of the damaged substrate layer, which is accompanied by a decrease in roughness. The increase in the layer thickness is observed due to the presence of etching residues at a further increase in the etching time from 4 to 12 s.

Subsequently, the samples were annealed at 350°C (heating time 1.5 h, exposure at 350°C for 5 min) and subsequent cooling to room temperature (25°C) with air input into the thermal vacuum cell. The experimental reflectometry curves (Figs. 3c, 3d) are described well by a simplified model: a substrate without additional sublayers, which indicates that the

damaged layer was removed by etching, and the layer of the etching residues evaporated after annealing. Table 5 shows the root-mean-square roughness of the substrates after etching, annealing at 350°C and subsequent cooling. After annealing, the surface roughness

Table 4. Parameters of the model of the layer on the substrate surface at 25°C after etching

Etching time, s	d , nm	ρ_e	σ_z , nm	χ^2
2	1.2	0.57	0.60	1.3
4	0.7	0.77	0.42	1.4
6	0.9	0.50	0.31	1.2
12	1.1	0.73	0.38	2.2

d is the layer thickness, ρ_e is the electron density of the layer relative to the substrate, σ_z is the surface-layer roughness.

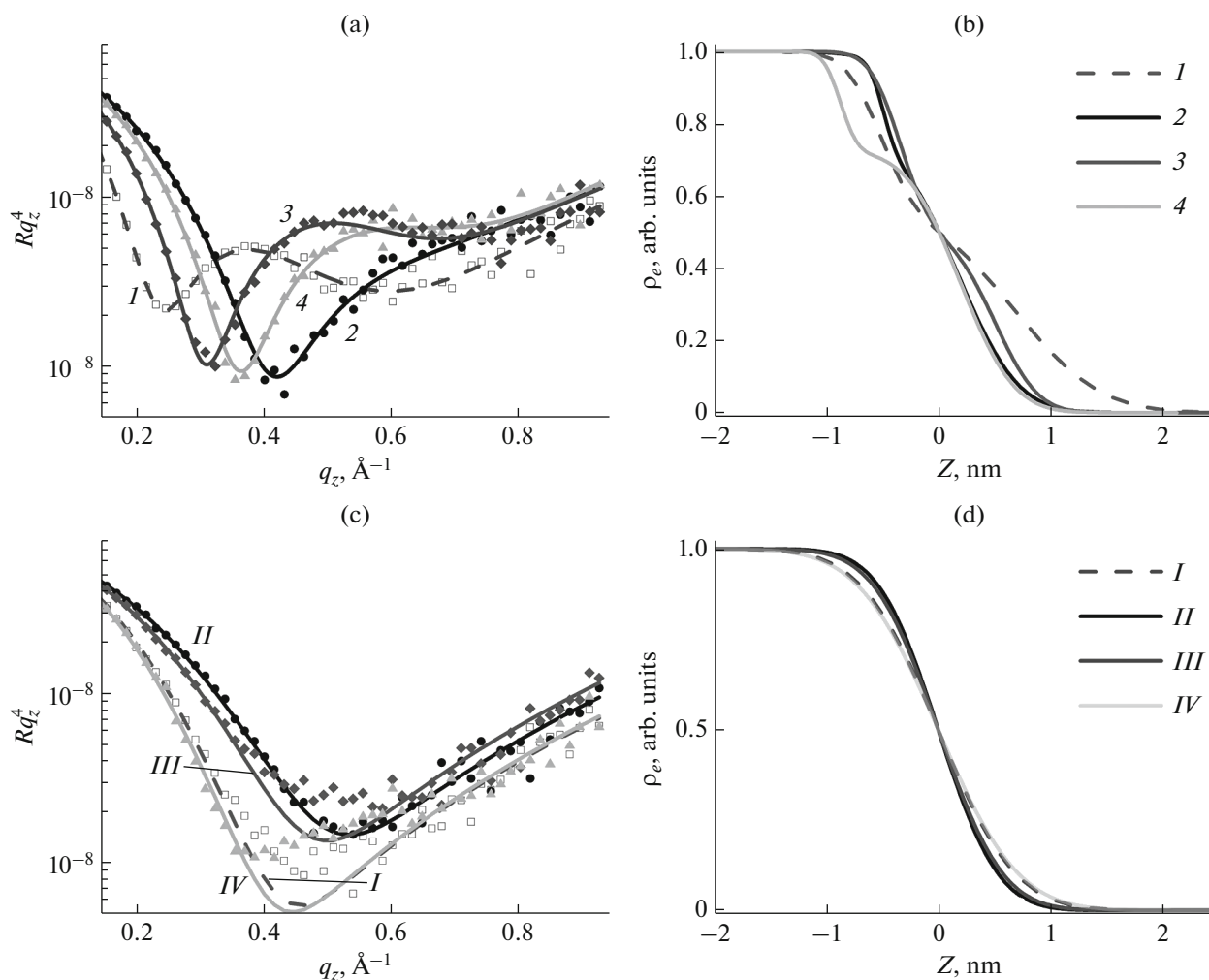


Fig. 3. Research results upon etching and subsequent vacuum annealing up to 350°C: (a, c) X-ray reflectometry curves; (b, d) corresponding electron density profiles over the sample depth after etching for 2 (I, *I*), 4 (2, *II*), 6 (3, *III*) and 12 s (4, *IV*) obtained at room temperature (*I–4*) and after heating and cooling to room temperature (*I–IV*). For clarity, the X-ray reflectometry curves are normalized to q_z^4 . Points—experiment, lines—calculation.

of the samples etched for 2 and 4 s decreases, which can be explained by the evaporation of residues of the etchant aqueous solution. The roughness increases in the samples with an etching time of 6 and 12 s, which is possibly due to the removal of a layer with a thickness of more than 1.5 nm and the formation of voids due to nonuniform etching of the silicon surface.

Table 5. Root-mean-square roughness of substrates (σ_z) after etching, annealing at 350°C and subsequent cooling

Etching time, s	σ_z , nm	χ^2
2	0.54	2.7
4	0.42	1.8
6	0.45	2.9
12	0.56	4.1

The X-ray reflectometry data show that the optimal etching time of the studied samples is 4 s—the lowest substrate roughness and the sharpest interface are observed (Figs. 3a, 3b, Table 5). As a result, after etching and annealing, it is possible to obtain a substrate with a roughness of 0.42 nm, free from impurity and organic contaminants, and to remove the surface layer observed in the samples of silicon wafers before etching (Figs. 3c, 3d, Table 5). It should be noted that the electron density of the substrates after etching for 2 and 12 s and annealing at 350°C is noticeably lower than that at an etching duration of 4 and 6 s. The electron density profile has more “blurred” interfaces in the first case compared to that in the second case.

CONCLUSIONS

The effect of vacuum annealing, cleaning in an ultrasonic bath and etching of the surface of silicon

substrates on the structure of the surface layer has been studied by the method of X-ray reflectometry. It has been shown that preliminary cleaning in an ultrasonic bath without subsequent annealing removes organic impurities readily soluble in ethanol, but increases the surface-layer roughness of the substrate by 0.05 nm. Annealing at a temperature of 150°C evaporates the water component of the surface layer and makes it possible to obtain a substrate surface with a roughness of 0.28 nm. Annealing at a temperature of 350°C additionally cleans the surface from heavier (mainly organic) contaminants and makes it possible to reveal a damaged surface layer 1.5 nm thick with a roughness of 0.3 nm.

The use of the surface treatment of silicon wafers in the form of etching at a rate of 1 nm/s for 4 s and subsequent annealing at 350°C makes it possible to fabricate a cleaned substrate without a surface layer with a roughness of 0.42 nm.

Silicon substrates with a surface modified in the above manner can be used for the deposition and study of organic and hybrid planar nanosystems (including weakly scattering X-ray radiation), which will improve the accuracy of determining the parameters of their layered structure and allow study of the effect of the substrate layer on the formation of thin films.

FUNDING

This work was supported by the Ministry of Science and Higher Education of the Russian Federation within the State Assignment of the Federal Research Center “Crystallography and Photonics” of the Russian Academy of Sciences using equipment of the Center for Collective Use (project RFMEFI62119X0035) in terms of preparing samples and implementing experiments, as well as supported by the Russian Foundation for Basic Research (project no. 19-29-12043 MK) in terms of the development of computational methods for the analysis of X-ray data.

REFERENCES

1. M. Morita, T. Ohmi, E. Hasegawa, M. Kawakami, and M. Ohwada, *J. Appl. Phys.* **68**, 1272 (1990).
2. D. Bauza, *Handbook of Surfaces and Interfaces of Materials* (Academic, New York, 2001), p. 115.
3. W. E. Wallace, W. L. Wu, and R. A. Carpio, *Thin Solid Films* **280**, 37 (1996).
4. C. Teichert, J. F. MacKay, D. E. Savage, M. G. Lagally, M. Brohl, and P. Wagner, *Appl. Phys. Lett.* **66**,

2346 (1995).

<https://doi.org/10.1063/1.113978>

5. S. K. Sinha, *Curr. Opin. Solid State Mater. Sci.* **1**, 645 (1996).
6. A. E. Blagov, A. L. Vasiliev, A. S. Golubeva, I. A. Ivanov, O. A. Kondrat'ev, Yu. V. Pisarevsky, M. Yu. Presnyakov, P. A. Prosekov, and A. Yu. Seregin, *Crystallogr. Rep.* **59**, 315 (2014).
<https://doi.org/10.1134/S1063774514030043>
7. A. E. Blagov, G. B. Galiev, R. M. Imamov, E. A. Klimov, O. A. Kondrat'ev, Yu. V. Pisarevskii, P. A. Prosekov, S. S. Pushkarev, A. Yu. Seregin, and M. V. Koval'chuk, *Crystallogr. Rep.* **62**, 355 (2017).
<https://doi.org/10.1134/S1063774517030026>
8. M. V. Kovalchuk, A. S. Boikova, Yu. A. D'yakova, M. A. Marchenkova, A. M. Opolchentsev, Yu. V. Pisarevskii, P. A. Prosekov, and A. Yu. Seregin, *Crystallogr. Rep.* **62**, 632 (2017).
<https://doi.org/10.1134/S1063774517040125>
9. A. E. Blagov, Yu. A. Dyakova, M. V. Kovalchuk, V. G. Kon, M. A. Marchenkova, Yu. V. Pisarevskii, and P. A. Prosekov, *Crystallogr. Rep.* **61**, 362 (2016).
<https://doi.org/10.1134/S1063774516030044>
10. A. Alekseev, P. Ihalainen, A. Ivanov, I. Domnin, E. Rosqvist, H. Lemmetyinen, E. Vuorimaa-Laukkanen, J. Peltonen, and S. Vyaz'min, *Thin Solid Films* **645**, 108 (2018).
<https://doi.org/10.1016/j.tsf.2017.10.018>
11. A. S. Boikova, Yu. A. D'yakova, K. B. Il'ina, M. A. Marchenkova, A. Yu. Seregin, P. A. Prosekov, Yu. A. Volkovskii, Yu. V. Pisarevskii, and M. V. Koval'chuk, *Crystallogr. Rep.* **63**, 719 (2018).
12. M. S. Folomeshkin, A. S. Boikova, Yu. A. Volkovsky, M. A. Marchenkova, P. A. Prosekov, and A. Yu. Seregin, *Crystallogr. Rep.* **65**, 827 (2020).
13. M. V. Kovalchuk, A. S. Boikova, Yu. A. Dyakova, K. B. Ilina, P. V. Konarev, M. A. Marchenkova, Yu. V. Pisarevskiy, P. A. Prosekov, A. V. Rogachev, and A. Yu. Seregin, *Thin Solid Films* **677**, 13 (2019).
14. Y. Hou, N. Jaffrezic-Renault, C. Martelet, C. Tlili, A. Zhang, J.-C. Pernollet, L. Briand, G. Gomila, A. Errachid, J. Samitier, L. Salvagnac, B. Torbiero, and P. Temple-Boyer, *Langmuir* **21**, 4058 (2005).
<https://doi.org/10.1021/la0471801>
15. W. Kern, *J. Electrochem. Soc.* **137**, 1887 (1990).
16. Telekom STV. www.telstv.ru/?page=ru_silicon_wafers.
17. L. G. Parratt, *Phys. Rev.* **95**, 359 (1954).
18. D. W. Marquardt, *J. Soc. Ind. Appl. Math.* **11**, 431 (1963).

Translated by L. Mosina